ChemComm

Accepted Manuscript

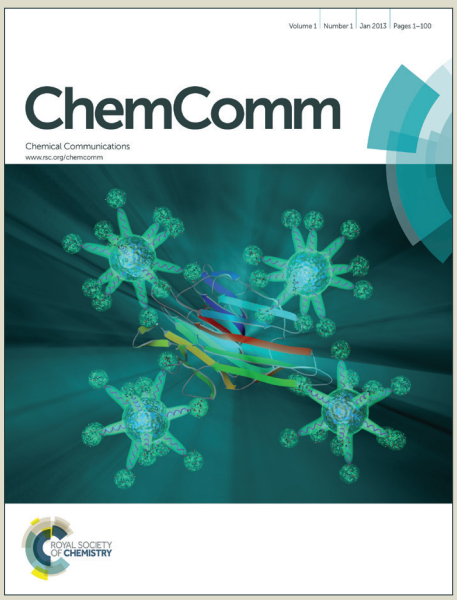

ROYAL SOCIETY OF CHEMISTRY

www.rsc.org/chemcomm

ChemComm

RSCPublishing

COMMUNICATION

Refractive index dependent real-time plasmonic nanoprobes on single silver nanocube for ultrasensitive detection of the lung cancer-associated miRNAs

Cite this: DOI: 10.1039/xoxxoooooox

Received ooth August 2014,
Accepted ooth August 2014

DOI: 10.1039/xoxxoooooox

www.rsc.org/

Lei Zhang,[a, ‡] Ying Zhang,[a, ‡] Yanling Hu,[a] Quli Fan,[a] Wenjing Yang,[a] Anran Li,[c] Shuzhou Li,[*c] Wei Huang[*ab] and Lianhui Wang[*a]

We developed a novel method for the real-time monitor of the delicate change in refractive index (RI) when DNA or RNA hybridize near DNA-capped silver nanocubes (AgNCs) surface. This method offers an alternative platform in quantitative analysis of the trace lung cancer-associated miRNAs in label-free detection.

For tumor diagnosis, detection of tumor biomarkers, such as protein, DNA and RNA, has shown higher sensitivity than traditional analysis methods. MicroRNAs (miRNAs), which act as tumor suppressors and display expression levels to predict human metastasis, can serve as biomarkers for diagnosis and therapy.1 The miR-21 has been found in specimens of many human cancers, especially those of lung cancer.2 As an oncomiR, its overexpression leads to tumor development and progression.1d Therefore, a novel analytical method with low limit of detection (LOD) has to be developed for the rapid detection of trace miR-21 for early diagnosis of lung cancer. It has been reported that there would be a notable change of refractive index (RI) from 1.37 to 1.75 after the nucleic acids hybridization.3 The RI changes on plasmonic structure surface can directly lead to a red-shift of the LSPR scattering peak position, which makes it possible to achieve a highly sensitive detection of DNA or RNA on a suitable metal nanoparticle (MNP). Therefore, plasmonic probes with high performance provide an alternative method for rapid and quantitative detection of trace nucleic acids molecules.

White light incident on a MNP induces the surface free electrons to oscillate collectively with a certain resonant frequency, which mainly depends on the MNP's size, shape, composition as well as the local environment.[4] Moreover, the scattered light is so intense that single MNP can be easily observed using dark-field microscopy (DFM). The plasmonic analytical nanotechnology, mainly depended on the coupling effect between different nanoparticles or the plasmon resonance energy transfer effects, has been a promising means in trace analysis of small molecules on a single particle surface, such as H_2S, NADH, Cu^{2+}, *et al.*[4c,5] Besides, DNA immobilized on the surfaces of gold nanoparticles had an enormous impact in the scattering spectrum. On one hand, the localized surface plasmon resonance (LSPR) scattering wavelength of individual Au-DNA conjugates is dependent on the length of the DNA change by endonuclease reactions[6]; on the other hand, the LSPR scattering peak positions would red-shift notably when the RI of local environment near the noble metals increased either in different solutions[7] or on different substrates.[8]

Silver nanocubes (AgNCs) with well-defined and controllable shapes, have attracted intensive attention in recent years because of their unique shape-dependent optical properties. They have been employed as near-field optical probes, and contrast agents for biomedical detection and have shown potential applications including catalysis, photonics, and data storage.[9] It is relatively straightforward to fabricate suitable plasmonic structures for promising usage in optical biosensors. For example, cubic silver nanoparticles with an average edge size of 55 nm exhibit much higher surface plasmon resonance (SPR) capability than silver nanoplates with the same size.[10] Distance depended coupling effects in two silver nanoparticles made a greater red-shift than gold nanoparticles.[11] And the plasmonic structures with special shape would be more sensitivity to the change of the interface microenvironment on nanoparticle surface.[12]

In this paper, the thiolated single-stranded DNA (ssDNA) molecular with specific DNA sequences, acting as the probe moleculars, were then modified on the surface of AgNCs which immobilized on glass slide surface. When the hybridization occurred between ssDNA molecular and miR-21, the LSPR scattering spectrum peak of AgNCs red-shifted depended on the concentration of target molecules, indicating an increase in the RI near Ag due to the higher refractive index of RNA than water. And the extraordinary sensing ability of single AgNC for the detection of target molecules (miR-21) was demonstrated. To the best of our knowledge, for the first time, we experimentally observed the real-time LSPR scattering optical response of nucleic acid hybridization process in situ on a single AgNC surface. In addition, finite-difference time-domain (FDTD) simulations were performed to verify the sensing mechanism of AgNCs. The good agreement between simulation results and experimental results indicates that the red shift of resonance position is caused by the RI change of the dielectric film formed at the AgNC surface due to DNA and RNA hybridization.

As illustrated in Fig. 1a, the single-AgNC plasmonic probes were successfully fabricated through assembly of ssDNA on the surface of AgNCs (a-II) (see the Supporting Information for more details).

Compared with the UV-Vis absorption spectra of AgNCs solution, the single nanoparticle scattering spectra showed a large red-shift after immobilizing on the ITO glass slide (Fig. S1 and Fig. 1f). This result was attributed to the high RI of ITO glass medium, which is consistent with a statistical analysis and FDTD calculations.[8] With overnight treatment of ssDNA solution, every AgNC surface could link large amount of ssDNA molecules, about 1150 molecules as calculated according to Mirkin's results.[13] A thin compact film composed of ssDNA and H_2O molecule formed, and the RI value of this film was between that of ssDNA and water (a-II). After 120 min treatment with miR-21 (a-III), the LSPR scattering spectra peak (λ_{max}) of AgNC@ssDNA probes red-shifted to longer wavelength and the DFM images showed a color transition from cyan (Fig. 1b-II) to dark green (b-III). The time-dependent LSPR scattering λ_{max} shift on a selected single AgNC@ssDNA probe was shown in Fig. S2 (ESI†). The typical AgNC@ssDNA probe's λ_{max} red-shifted continuously, and then got to the max peak-shift located about 518 nm at 2 h after adding 1 pM miR-21. These results might be conjectured to be caused by the delicate change of RI when the miRNAs take place of H_2O molecules between the DNA arrays (Fig. 1a).

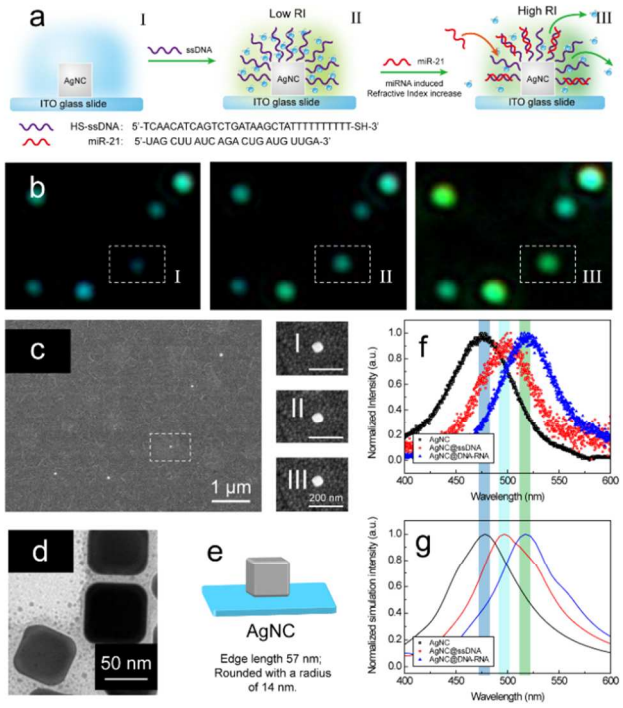

Fig. 1 a) Bio-sensing scheme of a AgNC@ssDNA probe based on the RI increase induced by hybridization at the single AgNC surface. b) Typical DFM images of AgNCs (b-I), AgNC@ssDNA (b-II), and AgNC@DNA-miRNA (b-III) on ITO glass slide. c) In-situ SEM images of the selected AgNC (c-I), AgNC@ssDNA (c-II), and AgNC@DNA-miRNA (c-III) in b). d) Typical TEM images of silver nanocubes. e) Schematic illustration of the AgNC constructed in FDTD simulations. f) Corresponding LSPR scattering spectra of the selected AgNC, AgNC@ssDNA, and AgNC@DNA-miRNA in b). g) The simulated LSPR spectra of the model in a).

In order to demonstrate the role of RI change in miRNA sensing of single AgNC, FDTD simulations were carefully carried out.[14] In this study, DFM images, in-situ SEM images and LSPR scattering spectra (Fig. 1b, c, f) were employed for making a direct comparison with 3D FDTD calculated results (Fig. 1g). The good agreement between simulation results and experimental results indicates that the RI change could be used for designing novel plasmonic probes for biological-labeling and label-free detection with high sensitivity based on single AgNC.Fig. S3b (ESI †) shows the calculated electric field distributions ($|E|^2/|E_0|^2$) for silver nanocube (b-I), silver nanocube with 10 nm DNA layer (b-II) and silver nanocube with 10 nm DNA-miRNA layer (b-III) under their corresponding resonant wavelengths, respectively. The electric fields are both plotted at the plane 1 nm away from the cube surface. The results show that intense electric fields are distributed at the four corners of the nanocube, indicating that the red shift of the resonance peak is mainly caused by DNA or RNA adsorbed on the surface.

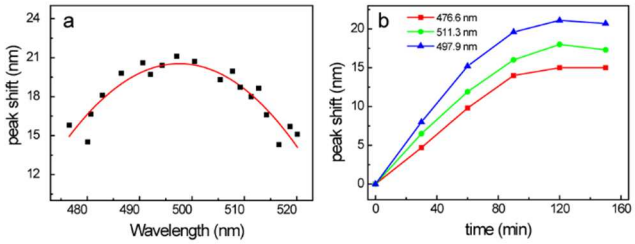

Fig. 2 a) Distribution curve corresponding to the $\Delta\lambda_{max}$ values of different sized ssDNA modified AgNCs treated with miR-21(1 PM) for 120 min. The red line is the Gaussian fit of the experimental data. b) Time-dependent spectral shifts of three different sized ssDNA modified AgNCs with $\Delta\lambda_{max}$ values of 476.6 nm (■), 497.9 nm (▲), and 511.3 nm (●) after treatment with miR-21(1 PM).

Although single MNP enables highly sensitive detection, the nanoparticle must be selected carefully to ensure sufficient signal intensity. Statistical analysis of the scattering spectra of a number of AgNC@ssDNA probes revealed that the initial peak position (λ_{max}) located at around 497 nm (the corresponding edge length of the AgNCs is about 55 nm) were significantly shifted with maximum value after the hybridization (Fig. 2a). The real-time processes of time-dependent spectral shifts of three ssDNA modified AgNCs in different sizes with present of miR-21 (1 pM) are shown in Fig. 2b. Each AgNC@ssDNA probe exhibited different red-shift ability, and the $\Delta\lambda_{max}$ up to 21 nm were observed after treatment with miR-21 for 2 h. This difference in $\Delta\lambda_{max}$ values can be attributed to variations in size or shape of AgNC, which was similar with our previous reports of Cu shell growth on single gold nanoparticle.[4c]

To determine the sensitivity of this method, the AgNC@ssDNA probes with initial scattering peak (λ_{max}) around 497 nm were employed for monitoring the hybridization process with different concentrations of miR-21 ranging from 1 fM to 1 nM. The recorded LSPR spectra peak position linearly shifted with the increase of miR-21 (Fig. 3a, b). As shown in Fig. 3c, a linear relationship between the $\Delta\lambda_{max}$ and the miR-21 concentration is observed. The LOD of this probe was calculated to 0.1 fM when the signal to noise ratio is 3. The successful analysis of miR-21 by the λ_{max} shift in the LSPR spectra exhibited higher sensitivity than previous reported biosensors on single nanoparticle level.[5c,15] After the hybrization process completed, the covered reaction sulotion on this miRNA biochip were changed to 90 ^{o}C water, the scattering spectra of AgNC@DNA-miRNA exhibited noteble blue-shift after removal of miR-21 on the nano-probe surface and was shown in Fig. S4. Fig. 3d showed the time-dependent spectral shifts of three typical AgNC@ssDNA probes with the initial scattering peak around 497 nm after adding different nucleic acid molecules (Table S1) with the same concentration. Compared with the results of the hybridization between ssDNA and miR-21, a scarcely red-shift of the scattering spectra by the hybridization between ssDNA and random miRNA is observed, and the change of LSPR spectra is smaller after addition of single-base mismatch miRNA. The hybridization between ssDNA and miRNA on AgNCs surface was completed after the match of each base pair for 2 h on a cleaned ITO glass slide.

In summary, we developed a novel method combining LSPR spectroscopy and DFM color images for the ultrasensitive detection

of the cancer-associated miRNAs on a single AgNC. As the concentration of miR-21 increases, the hybridization between ssDNA and miR-21 on AgNCs surface results in a color change in DFM and a linear red-shift of scattering peak. Time-dependent spectral shifts of the nanoprobes not only showed high selectivity towards the biomarker of lung cancer, but also displayed a good linearity in a wide dynamic range with a low LOD up to 0.1 fM. The experimental observations can be explained well via theoretical models by FDTD simulations. Accordingly, future efforts will be directed to characterize other specific binding processes of bio-markers in real sample using single plasmonic nanoparticle, which will be more valuable in combined detection of multiple biomarkers for early diagnosis of lung cancer.

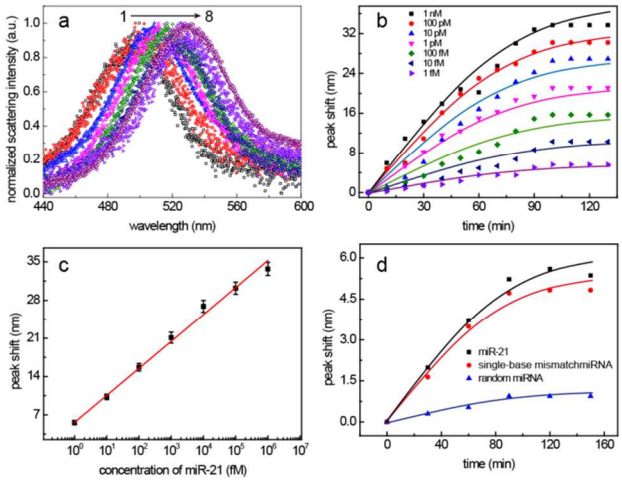

Fig. 3 a) Typical scattering spectra of AgNC@ssDNA probes before (1) and after treatment with 1, 10, 10^2, 10^3, 10^4, 10^5 and 10^6 fM miR-21 (2–8). b) Time-dependent spectral peak shifts in different concentrations corresponding to a). c) Relationship of peak shift in different concentrations of miR-21. d) The plots of three typical AgNCs probes' scattering spectra $\Delta\lambda_{max}$ versus time for AgNC@ssDNA probes under different interference conditions: 1, control (1 fM, ■); 2, single-base mismatch miRNA (1 fM, ●); 3, random miRNA (1 fM, ▲). The selected AgNCs probes' initial scattering λ_{max} located around 497 nm.

For the financial support for this work, we thank the State Plan for Development of Basic Research in Key Areas (2012CB933301), the Ministry of Education of China (IRT1148, NCET-10-0179), the National Natural Science Foundation of China (No. 61205195), the Specialized Research Fund for Doctoral College (20093223110003, 20123223120011, 20123223110007), the University Science Research Project of Jiangsu Province (12KJB150018, NY211049), the Open Research Fund of key state laboratory of Southeast University (BJ211029), Singapore Ministry of Education via Tier 2 Grant (MOE 2011-T2-2-085).

Notes and references

[a] Key Laboratory for Organic Electronics & Information Displays (KLOEID) and Institute of Advanced Materials (IAM), Nanjing University of Posts & Telecommunications, Nanjing 210023, P. R. China. E-mail: iamlhwang@njupt.edu.cn

[b] Jiangsu-Singapore Joint Research Center for Organic/Bio- Electronics & Information Displays and Institute of Advanced Materials, Nanjing Tech University, Nanjing 211816, P. R. China.

E-mail: iamwhuang@njupt.edu.cn

[c] Division of Materials Science, School of Materials Science and Engineering, Nanyang Avenue, 639798, Singapore.

E-mail: lisz@ntu.edu.sg

‡These authors contributed equally to this paper.

† Electronic Supplementary Information (ESI) available: Experimental Details: AgNCs synthesis, Modification procedure, analysis methods, single nanoparticle DFM imaging, scattering spectroscopy collection, and FDTD simulation. See DOI: 10.1039/c000000x/

1 (a) J. Lu, G. Getz, E. A. Miska, E. Alvarez-Saavedra, J. Lamb, D. Peck, A. Sweet-Cordero, B. L. Ebert, R. H. Mak and A. A. Ferrando, *Nature* 2005, **435**, 834; (b) K. J. Png, N. Halberg, M. Yoshida and S. F. Tavazoie, *Nature* 2012, **481**, 190; (c) Y. Wang, G. Chen, M. X. Yang, G. Silber, S. X. Xing, L. H. Tan, F. Wang, Y. H. Feng, X. G. Liu, S. Z. Li and H. Y. Chen, *Nat. Commun.* 2010, **1**, 87; (d) L. Yu, N. W. Todd, L. X. Xing, Y. Xie, H. Zhang, Z. Q. Liu, H. B. Fang, J. A. Zhang, R. L. Katz and F. Jiang, *Int. J. Canc.* 2010, **127**, 2870; (e) S. Volinia, G. A. Calin, C.-G. Liu, S. Ambs, A. Cimmino, F. Petrocca, R. Visone, M. Iorio, C. Roldo, M. Ferracin, R. L. Prueitt, N. Yanaihara, G. Lanza, A. Scarpa, A. Vecchione, M. Negrini, C. C. Harris and C. M. Croce, *P. Natl. Acad. Sci.* 2006, **103**, 2257; (f) F. Degliangeli, P. Kshirsagar, V. Brunetti, P. P. Pompa and R. Fiammengo, *J. Am. Chem. Soc.* 2014, **136**, 2264; (g) B. P. Maliwal, J. Kusba and J. R. Lakowicz, *Biopolymers* 1995, **35**, 245.

2 (a) I. A. Asangani, S. A. K. Rasheed, D. A. Nikolova, J. H. Leupold, N. H. Colburn, S. Post and H. Allgayer, *Oncogene* 2008, **27**, 2128; (b) S. Volinia, G. A. Calin, C. G. Liu, S. Ambs, A. Cimmino, F. Petrocca, R. Visone, M. Iorio, C. Roldo, M. Ferracin, R. L. Prueitt, N. Yanaihara, G. Lanza, A. Scarpa, A. Vecchione, M. Negrini, C. C. Harris and C. M. Croce, *P. Natl. Acad. Sci.* 2006, **103**, 2257.

3 (a) A. J. Steckl, *Nat. Photon.* 2007, **1**, 3; (b) J. Zhu, J. J. Li and J. W. Zhao, *Appl. Surf. Sci.* 2013, **275**, 264; (c) A. Tane, F. Kajzar, R. Zgarian, I. Rau, D. Grabarek, P. Karpinski and A. Miniewicz, *Macromol. Res.* 2013, **21**, 331; (d) K. H. Su, Q. H. Wei, X. Zhang, J. J. Mock, D. R. Smith and S. Schultz, *Nano Lett.* 2003, **3**, 1087.

4 (a) C. L. Haynes and R. P. Van Duyne, *J. Phys. Chem. B* 2001, **105**, 5599; (b) C. Novo, A. M. Funston, A. K. Gooding and P. Mulvaney, *J. Am. Chem. Soc.* 2009, **131**, 14664; (c) L. Zhang, Y. Li, D.-W. Li, C. Jing, X. Chen, M. Lv, Q. Huang, Y.-T. Long and I. Willner, *Angew. Chem. Int. Ed.* 2011, **50**, 6789.

5 (a) C. Novo, A. M. Funston and P. Mulvaney, *Nat. Nanotechnol.* 2008, **3**, 598; (b) L. Shi, C. Jing, W. Ma, D. W. Li, J. E. Halls, F. Marken and Y. T. Long, *Angew. Chem. Int. Ed.* 2013, **52**, 6011; (c) B. Xiong, R. Zhou, J. R. Hao, Y. H. Jia, Y. He and E. S. Yeung, *Nat. Commun.* 2013, **4**.

6 G. L. Liu, Y. D. Yin, S. Kunchakarra, B. Mukherjee, D. Gerion, S. D. Jett, D. G. Bear, J. W. Gray, A. P. Alivisatos, L. P. Lee and F. Q. F. Chen, *Nat. Nanotechnol.* 2006, **1**, 47.

7 (a) A. D. McFarland and R. P. Van Duyne, *Nano Lett.* 2003, **3**, 1057; (b) J. J. Mock, D. R. Smith and S. Schultz, *Nano Lett.* 2003, **3**, 485.

8 E. Ringe, J. M. McMahon, K. Sohn, C. Cobley, Y. N. Xia, J. X. Huang, G. C. Schatz, L. D. Marks and R. P. Van Duyne, *J. Phys. Chem. C* 2010, **114**, 12511.

9 (a) Q. Zhang, N. Li, J. Goebl, Z. Lu and Y. Yin, *J. Am. Chem. Soc.* 2011, **133**, 18931; (b) Y. Xiong, I. Washio, J. Chen, M. Sadilek and Y. Xia, *Angew. Chem. Int. Ed.* 2007, **46**, 4917; (c) J. Zeng, J. Tao, D. Su, Y. Zhu, D. Qin and Y. Xia, *Nano Lett.* 2011, **11**, 3010; (d) Y. G. Sun and Y. N. Xia, *Adv. Mater.* 2003, **15**, 695.

10 (a) D. Yu and V. W.-W. Yam, *J. Am. Chem. Soc.* 2004, **126**, 13200; (b) D. B. Yu and V. W. W. Yam, *J. Phys. Chem. B* 2005, **109**, 5497; (c) Y. Sun and C. Lei, *Angew. Chem. Int. Ed.* 2009, **48**, 6824.

11 C. Sonnichsen, B. M. Reinhard, J. Liphardt and A. P. Alivisatos, *Nat. Biotechnol.* 2005, **23**, 741.

12 K. A. Willets and R. P. Van Duyne, *Annu. Rev. Phys. Chem.* 2007, **58**, 267.

13 S. J. Hurst, A. K. R. Lytton-Jean and C. A. Mirkin, *Anal. Chem.* 2006, **78**, 8313.

14 (a) A. Taflove and S. C. Hagness *Computational electrodynamics*; Artech house Boston, 2000; (b) S. Pedireddy, A. R. Li, M. Bosman, I. Y. Phang, S. Z. Li and X. Y. Ling, *J. Phys. Chem. C* 2013, **117**, 16640.

15 (a) S. K. Dondapati, T. K. Sau, C. Hrelescu, T. A. Klar, F. D. Stefani and J. Feldmann, *Acs Nano* 2010, **4**, 6318; (b) A. R. Halpern, J. B. Wood, Y. Wang and R. M. Corn, *Acs Nano* 2014, **8**, 1022.

